Journal of Neonatal Surgery
ISSN(Online): 2226-0439
Vol. 14, Issue 32s (2025)
https://www.jneonatalsurg.com

OPEN ACCESS

Isolation and Structural Characterization of Ursolic Acid from Medicinal Plant Extract and Its In Silico Inhibitory Potential Against Inflammation-Linked Molecular Targets

P. Senthil Kumar*[1], Vinciya T[2]

[1]Department of Pharmaceutical Chemistry, Faculty of Pharmacy, Dr. M.G.R Educational and Research Institute, Chennai-600077.
[2]Department of Pharmacology, Faculty of Pharmacy, Dr. M.G.R Educational and Research Institute, Chennai-600077.
***Corresponding Author**
email ID:senthilbssk@gmail.com

Cite this paper as: P. Senthil Kumar, Vinciya T (2025) Isolation and Structural Characterization of Ursolic Acid from Medicinal Plant Extract and Its In Silico Inhibitory Potential Against Inflammation-Linked Molecular Targets. *Journal of Neonatal Surgery*, 14 (32s), 6024-6040.

ABSTRACT

Objectives: The study aimed to isolate, characterize, and evaluate the neuroprotective and anti-inflammatory potential of a phytochemical compound from a medicinal plant. The primary objective was to assess the binding affinity of ursolic acid, a pentacyclic triterpenoid, against Alzheimer's disease-relevant protein targets using molecular docking. This included enzymes known to contribute to neuroinflammation and amyloid-beta processing, which are implicated in Alzheimer's pathology.

Methods: The crude methanolic extract of the plant was subjected to gradient silica gel column chromatography, followed by purification and recrystallization, yielding a single pure compound. The structure of this compound was confirmed as ursolic acid using FTIR, ^{1}H-NMR, ^{13}C-NMR, and mass spectrometry. Molecular docking was then performed using AutoDock Vina to explore the interaction of ursolic acid with three Alzheimer's-linked targets:

- Glycogen Synthase Kinase-3β (GSK-3β; PDB ID: 1H8F)
- Angiotensin-Converting Enzyme (ACE; PDB ID: 1O86)
- TNF-α Converting Enzyme (TACE; PDB ID: 3LOT)

These proteins were prepared by removing heteroatoms and adding polar hydrogens. Ursolic acid was modeled and energy-minimized using ChemSketch and UCSF Chimera. Binding interactions were visualized using Discovery Studio.

Result:Ursolic acid exhibited favorable binding affinities to all three protein targets involved in neuroinflammation and Alzheimer's progression. The docking results demonstrated stable hydrogen bonding and hydrophobic interactions at the active sites of GSK-3β (linked to tau phosphorylation), ACE (implicated in neurovascular dysfunction), and TACE (key in neuroinflammation via TNF-α activation). The strongest binding affinity was observed with TACE, indicating ursolic acid's potential in modulating inflammatory cytokine release. These findings suggest that ursolic acid could attenuate both amyloid and inflammatory pathways in Alzheimer's pathology.

Conclusion: This multi-approach study confirmed the identity of ursolic acid and validated its multi-target inhibitory potential against key Alzheimer's disease-related enzymes. The compound's strong binding affinity, particularly toward TACE and GSK-3β, supports its possible use in modulating neuroinflammation, amyloid cascade, and tau hyperphosphorylation, which are hallmarks of Alzheimer's disease. The study underscores the relevance of plant-derived compounds like ursolic acid in neurodegenerative drug discovery, and supports molecular docking as a predictive tool for evaluating neuroprotective leads

Keywords: *Ursolic acid; Molecular docking; GSK3; ACE; TACE; Phytochemical isolation; NMR; Inflammation; AutoDock Vina; Drug discovery*

1. INTRODUCTION

Medicinal plants have served as a cornerstone of traditional medicine for centuries and continue to offer a rich reservoir of bioactive compounds for modern pharmaceutical development(1). Among the various classes of natural products, pentacyclic triterpenoids have been extensively studied for their multifaceted pharmacological activities(2). One such compound, ursolic acid, is a naturally occurring triterpenoid found in the leaves and peels of many medicinal plants, including Ocimum sanctum, Rosmarinus officinalis, and Eucalyptus globulus(3). Known for its wide spectrum of biological activities, including anti-

Chronic inflammatory diseases such as **rheumatoid arthritis, cardiovascular disease, neuroinflammation, and metabolic syndrome** are increasing globally and represent a significant burden on healthcare systems(5). These conditions are frequently associated with dysregulated immune responses and overexpression of key pro-inflammatory mediators and enzymes(6). Among these, **Glycogen Synthase Kinase-3 (GSK3)**, **Angiotensin-Converting Enzyme (ACE)**, and **Tumor Necrosis Factor-α Converting Enzyme (TACE)** play central roles(7). GSK3 is a serine/threonine kinase involved in numerous cellular pathways including those regulating inflammation, apoptosis, and immune response(8). ACE, beyond its classical role in blood pressure regulation, has been implicated in vascular inflammation and endothelial dysfunction(9). TACE (also known as ADAM17) is responsible for cleaving membrane-bound TNF-α, thus releasing its soluble form and contributing to the systemic inflammatory cascade(10).

Given the central role of these enzymes in inflammatory pathology, the development of small-molecule inhibitors targeting GSK3, ACE, and TACE holds considerable therapeutic promise(11). However, the high cost and time-intensive nature of traditional drug discovery necessitate the integration of **computational approaches**, such as **molecular docking**, to accelerate candidate screening and target validation(12). Molecular docking serves as a powerful in silico tool that predicts the preferred orientation of small molecules within the active sites of protein targets, allowing for the assessment of potential binding affinity and key interactions(13).

In the present study, we aimed to isolate and characterize bioactive constituents from a medicinal plant extract, followed by **computational evaluation of their anti-inflammatory potential(14)**. Using **gradient silica gel column chromatography**, a pure compound was successfully isolated and structurally elucidated via **Fourier-Transform Infrared (FT-IR) spectroscopy, Proton and Carbon Nuclear Magnetic Resonance (^{1}H-NMR and ^{13}C-NMR), and Mass Spectrometry (MS)**(15). The isolated compound was identified as **ursolic acid** based on its spectral characteristics and molecular weight(16). Subsequently, molecular docking studies were carried out using the crystal structures of **GSK3 (PDB ID: 1H8F), ACE (PDB ID: 1O86), and TACE (PDB ID: 3LOT)**, retrieved from the Protein Data Bank(17,18). The docking analysis was conducted using **AutoDock Vina integrated within UCSF Chimera**, focusing on key binding interactions and scoring functions to evaluate the compound's potential as a multi-target inhibitor(19,20).

This integrated experimental and computational approach not only facilitates the identification of novel plant-derived anti-inflammatory agents but also contributes to the rational design of lead compounds for further in vivo and clinical evaluation(21). Our findings support the potential role of **ursolic acid as a therapeutic candidate** for managing inflammation-driven diseases through simultaneous inhibition of GSK3, ACE, and TACE(22).

2. EXTRACTION METHOD:

Weigh about 200–500 g of the**sidamysorensis**powdered plant material.

Load the powder into a Soxhlet extractor.

Use analytical-grade chloroform (boiling point ~61.2 °C) as the extraction solvent.

Set the Soxhlet apparatus to reflux for 6–8 hours or until the siphoning becomes colorless.

This step allows for continuous extraction of non-polar to moderately polar phytoconstituents like alkaloids, flavonoids, sterols, and terpenoids.

After extraction, the chloroform extract is collected and filtered through Whatman No.1 filter paper.

Concentrate the filtrate using a **rotary evaporator** under reduced pressure at 40–45 °C to obtain a **semi-solid or gummy crude extract**.

Air-dry or vacuum-dry the concentrated extract completely to remove traces of chloroform.

Weigh and store the dried crude extract in a desiccator or airtight container at 4 °C.

3. MATERIALS & METHOD:

Melting point was determined by determined in open glass capillaries on SERVO melting point apparatus and were uncorrected. The FTIR spectra were obtained using KBr discs on Perkin Elmer FTIR spectrophotometer 1600(23). ^{1}H-NMR and ^{13}C-NMR spectra were recorded on JEOL spectrometer at 500MHz, respectively with DMSO-d*6* as solvent. Mass spectra were obtained using JEOL-Accu TOF JMS- T 100 LC Mass spectrometer(24). Column chromatography was carried out using silica gel 100-200 mesh (Merck), while TLC was carried out using silica gel 60PF254(25).

Isolation of active constituents:

The plant extract was dissolved in methanol and adsorbed in silica gel 60 – 120 mesh. The adsorbed extract was loaded into silica gel column (100 - 200 mesh size), which was previously packed with petroleum ether solvent(26).

The column was eluted with petroleum ether followed by gradually increasing polarity with petroleum ether: ethyl acetate

(90:10; 80:20; 70:30; 60:40; 50:50; 40:60; 30:70; 20:80; 10:90) and finally with 100% Ethylaceate. The column was further eluted with Ethylacetate: Chloroform (90:10; 80:20; 70:30; 60:40; 50:50; 30:70; 20:80) and finally with 100% chloroform. The column was further eluted with Chloroform:Methanol (99:1; 98:2; 97:3; 96:4; 95:5; 94:6; 92:8; 90:10; 88:12; 85:15; 80:20 and finally with 100% methanol). Total 76 Fractions were collected and monitored with TLC(27,28). The fraction number 16 - 21 shows single spot with similar Rf value (0.58).These fractions were combined and the solvent was evaporated under reduced pressure. The resulting crude solid was further treated with activated charcoal in hot ethanol and the filtrate was kept for crystallization. The resulting solid was submitted for Mass spectra, ^{13}C-NMR, ^{1}H-NMR, and FT-IR spectra analysis(29,30).

Compound-1:**colourless solid, m.p. 284 - 287 °C; $C_{30}H_{48}O_3$**

EI-MS **m/z: 457.3 (M+1)**

^{1}H-NMR (DMSO-***d6***):**δ ppm: 11.97 (s, 1H, -COOH); 5.12 – 5.15 (d, 1H, =CH); 4.28 – 4.29 (d, 1H, -OH); 2.97 – 2.99 (m, 1H, -CH); 2.09 – 2.17 (m, 1H, -CH); 1.77 – 1.84 (m, 3H, -CH); 1.37-1.67 (m, 10H, -CH, -CH_2); 1.23 – 1.31 (m, 6H, -CH_2); 1.09 – 1.14 (m, 1H, -CH); 1.01 – 1.04 (s, 3H, -CH_3); 0.80 – 0.97 (m, 14H, -CH_2, -CH_3); 0.67 – 0.74 (m, 6H, -CH_3)**

^{13}C-NMR (DMSO-***d6***):**δppm:178.56 (C-28), 138.17(C-13), 124.56 (C-12), 76.80 (C-3), 54.77(C-17), 52.35(C-178, 47.00 (C-9), 45.42(C-14), 41.62(C-19), 41.29 (C-20), 40.78 (C-7), 36.58(C-22), 32.82(C-21), 30.39(C-1), 29.04(C-2), 28.25(C-4), 27.52(C-10), 26.98(C-5), 25.58(C-23), 23.79(C-24), 22.83(C-19), 21.06(C-30), 17.99, 17.01, 16.89(C-29), 16.07(C-27), 15.21(C-26), 15.09(C-25)**

FT-IR (KBr cm-1): **3405 cm^{-1} (-COOH group); 2926 cm^{-1} (-CH stretch), 1688 cm^{-1} C=O; 1456 cm^{-1} (CH_2) ; 1030 (C-O).**

The ^{1}H-NMR spectrum showed dimethyl signals at δ 0.67 – 0.74 ppm. A doublet signals appeared at δ 5.12 – 5.15 was assigned to vinyl proton. Proton at δ 11.97 was assigned to carboxylic acid group. A multiplet signals at δ 0.80 – 0.97 were assigned to methine protons, suggesting triterpenoidal nature of the compound(31).

The ^{13}C-NMR spectrum showed 30 carbons which included hydroxy carbon at δ76.80, was characteristics of C-3 carbon attached with hydroxyl moiety. Two olefinic carbons appeared at δ138.17 and 124.56 which were identical with the chemical shift of C13 and C12 respectively. The signals showed at δC 16.07, 15.21, 15.09 typical of C-25, C-27 and C-26 of methyl groups respectively. The carboxylic group suggested by the ^{1}H-NMR spectrum was confirmed by the ^{13}C-NMR resonance observed at δ178.56(32).

The FTIR spectrum showed important absorptions attributable to carboxylic acid group at 3405 cm-1 and -CH stretch at 2926 cm-1. The other peaks are observed at 1688 cm-1 (conjugated C=O) and 1030 cm-1 (C–O)(33).

The molecular weight of the isolated compound determined by high-resolution mass spectrometry and the molecular ion peak appearing at m/z 457.3 (M+1)(34).

This pattern of the spectrum was identical with that of compound Ursolic acid [1]. The pentacyclic triterpenoidstructure of compound-1 as shown in Fig-1.

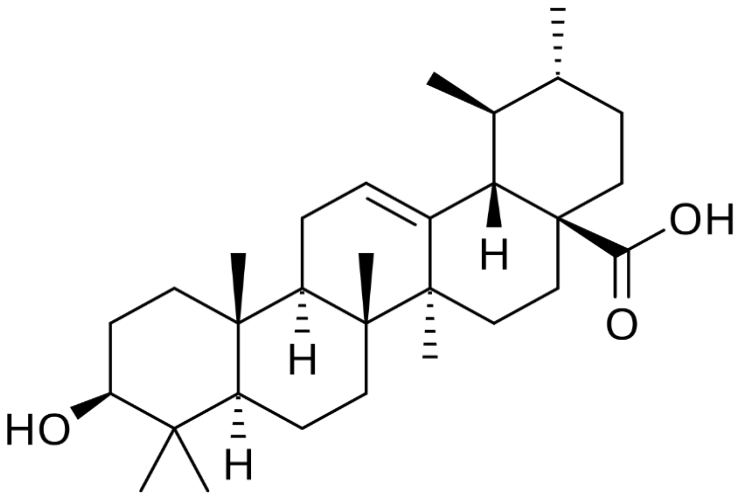

Fig-1.ursolic acid

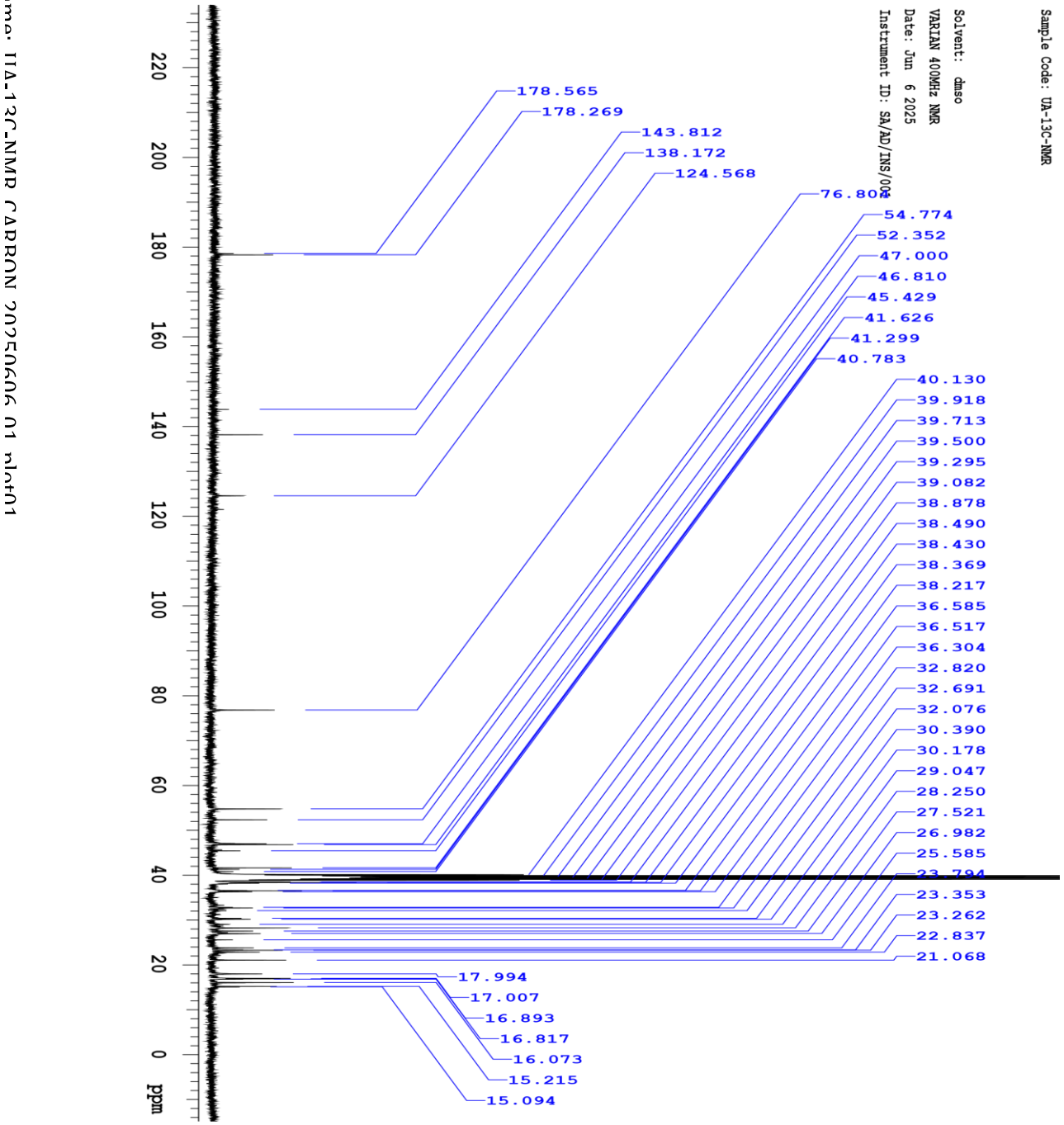

Sample Code: UA-13C-NMR

Solvent: dmso

VARIAN 400MHz NMR

Date: Jun 6 2025

Instrument ID: SA/AD/INS/001

Plotname: UA-13C-NMR_CARBON_20250606_01_plot02

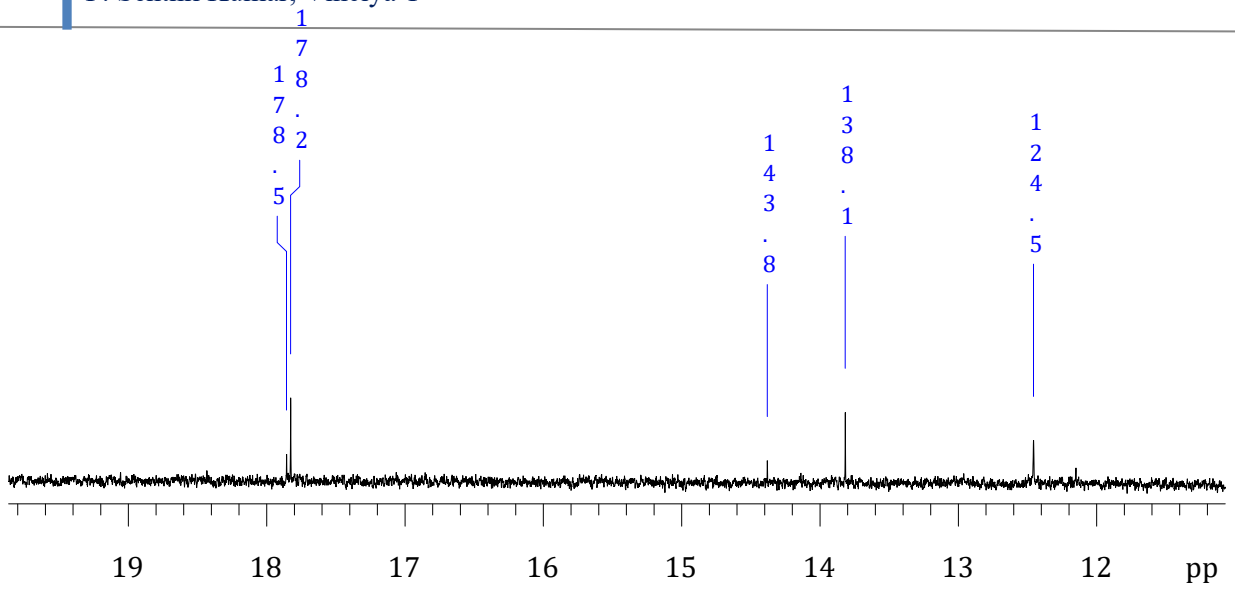

Plotname: UA-13C-NMR_CARBON_20250606_01_plot02

Verified by:KVS

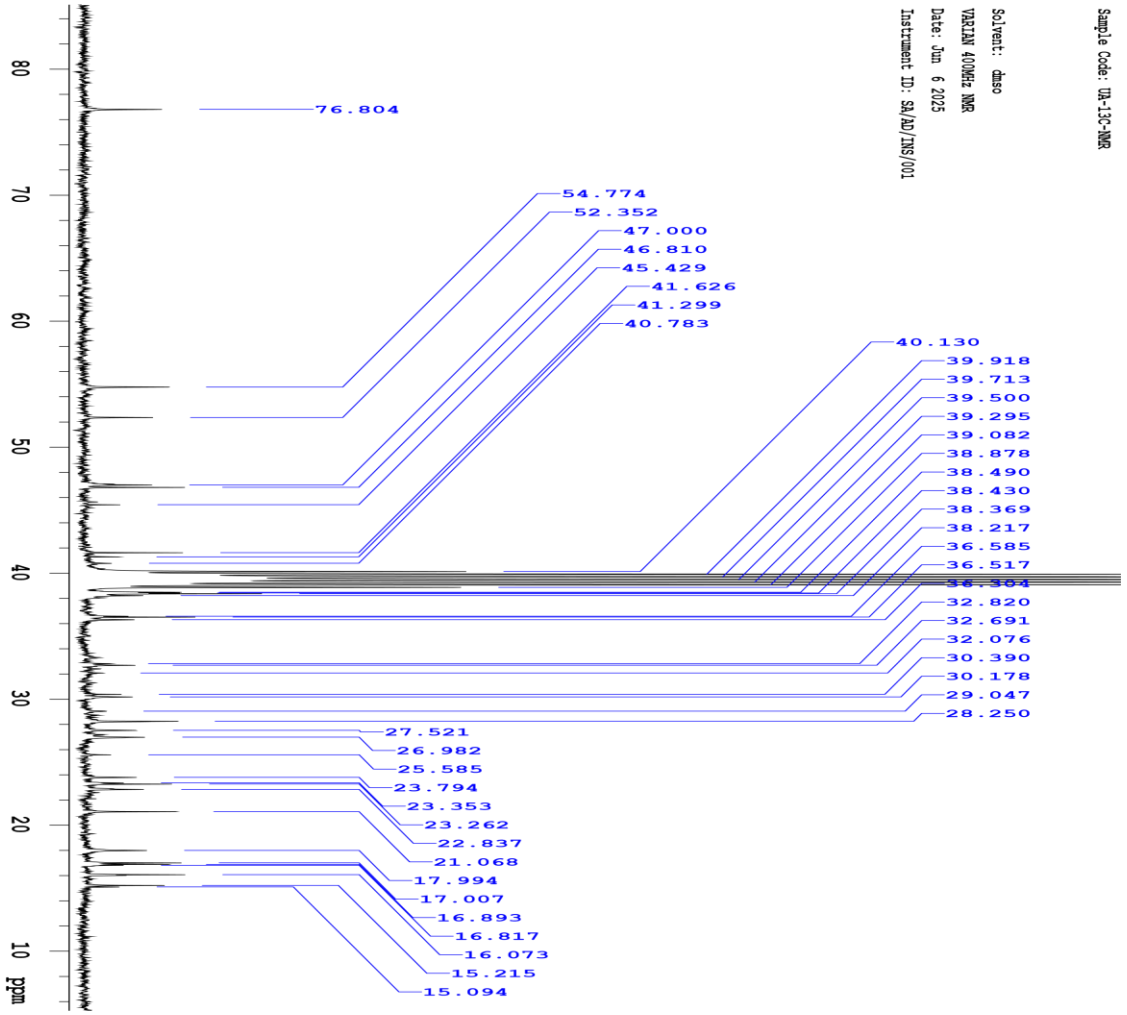

exp10 CARBON

SAMPLE PRESATURATION date Jun 62025 satmode n solvent dmso wet n file /home/varian/~ SPECIAL data/2025/Jun/UA-1~ temp not used 3C-NMR_20250606_01~ gain 30

/UA-13C-NMR_CARBON~ spin 0

_20250606_01.fid hst 0.008 ACQUISITION pw90 9.100 sw 25000.0 alfa 10.000 at 1.311 FLAGS np 65536 il n fb 17000 in n bs 4 dp y ss 8 hsnn d1 3.000 PROCESSING nt 2000 lb 2.00 ct 1216 fn not used TRANSMITTER DISPLAY tn C13 sp -1489.8 sfrq 100.513 wp 24999.2 tof 1530.4 rfl 5460.4 tpwr 56 rfp 3969.8 pw 4.550 rp 69.4 DECOUPLER lp 0 dn H1 PLOT dof 0 wc 268 dm yyysc 0 decwave w vs 349 dpwr 40 th 2 dmf 8850 nm ph

Plotname: UA-13C-NMR_CARBON_20250606_01_plot04 INDEX

No.	Frequency	PPM	Height
1	17946.1	178.565	3.6
2	17916.3	178.269	10.0
3	14453.4	143.812	2.9
4	13886.5	138.172	8.4
5	12519.3	124.568	5.2
6	7718.9	76.804	10.3
7	5504.9	54.774	11.2
8	5261.5	52.352	9.1
9	4723.6	47.000	9.0
10	4704.5	46.810	13.3
11	4565.7	45.429	4.7
12	4183.4	41.626	13.0
13	4150.6	41.299	4.6
14	4098.8	40.783	3.6
15	4033.1	40.130	50.5
16	4011.8	39.918	150.1
17	3991.2	39.713	296.1
18	3969.8	39.500	348.7
19	3949.2	39.295	294.1
20	3927.9	39.082	162.1
21	3907.3	38.878	49.8
22	3868.3	38.490	12.9
23	3862.2	38.430	12.6
24	3856.1	38.369	23.5
25	3840.9	38.217	7.8
26	3676.8	36.585	5.8
27	3670.0	36.517	14.7
28	3648.6	36.304	6.6
29	3298.4	32.820	3.5

30	3285.5	32.691	6.8
31	3223.7	32.076	2.5
32	3054.3	30.390	–
33	3032.9	30.178	6.4
34	2919.2	29.047	2.9
35	2839.1	28.250	12.3
36	2765.9	27.521	6.8
37	2711.7	26.982	8.0
38	2571.3	25.585	3.5
39	2391.3	23.794	6.9
40	2347.0	23.353	5.2
41	2337.9	23.262	11.6
42	2295.2	22.837	7.9
43	2117.4	21.068	12.1
44	1808.4	17.994	8.3
45	1709.2	17.007	12.8
46	1697.8	16.893	11.2
47	1690.2	16.817	5.2
48	1615.4	16.073	13.3
49	1529.2	15.215	10.6
50	1517.0	15.094	4.6

Plotname: UA_PROTON_20250605_01_plot01 Sample Code: UA

Solvent: dmso

VARIAN 400MHz NMR

Date: Jun 5 2025

Instrument ID : SA/AD/INS/001

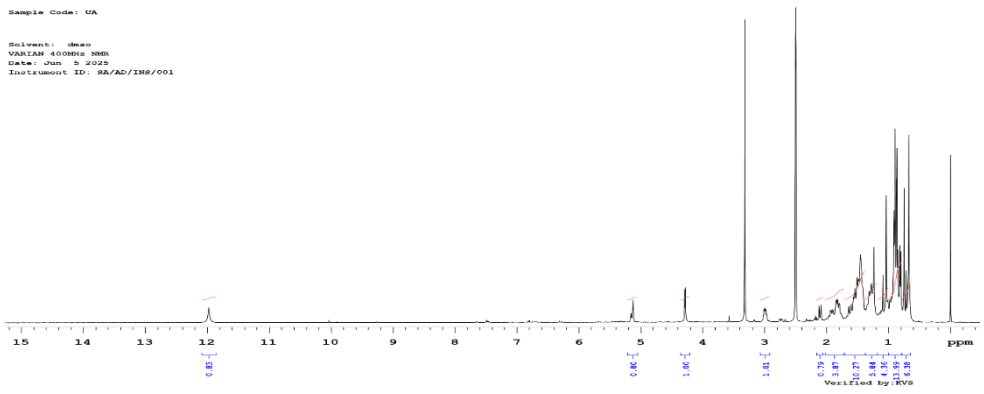

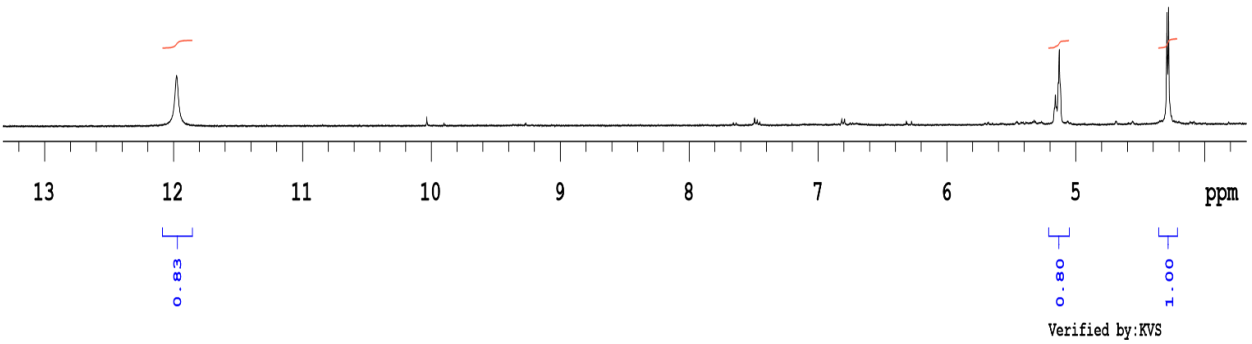

Plotname: UA_PROTON_20250605_01_plot02

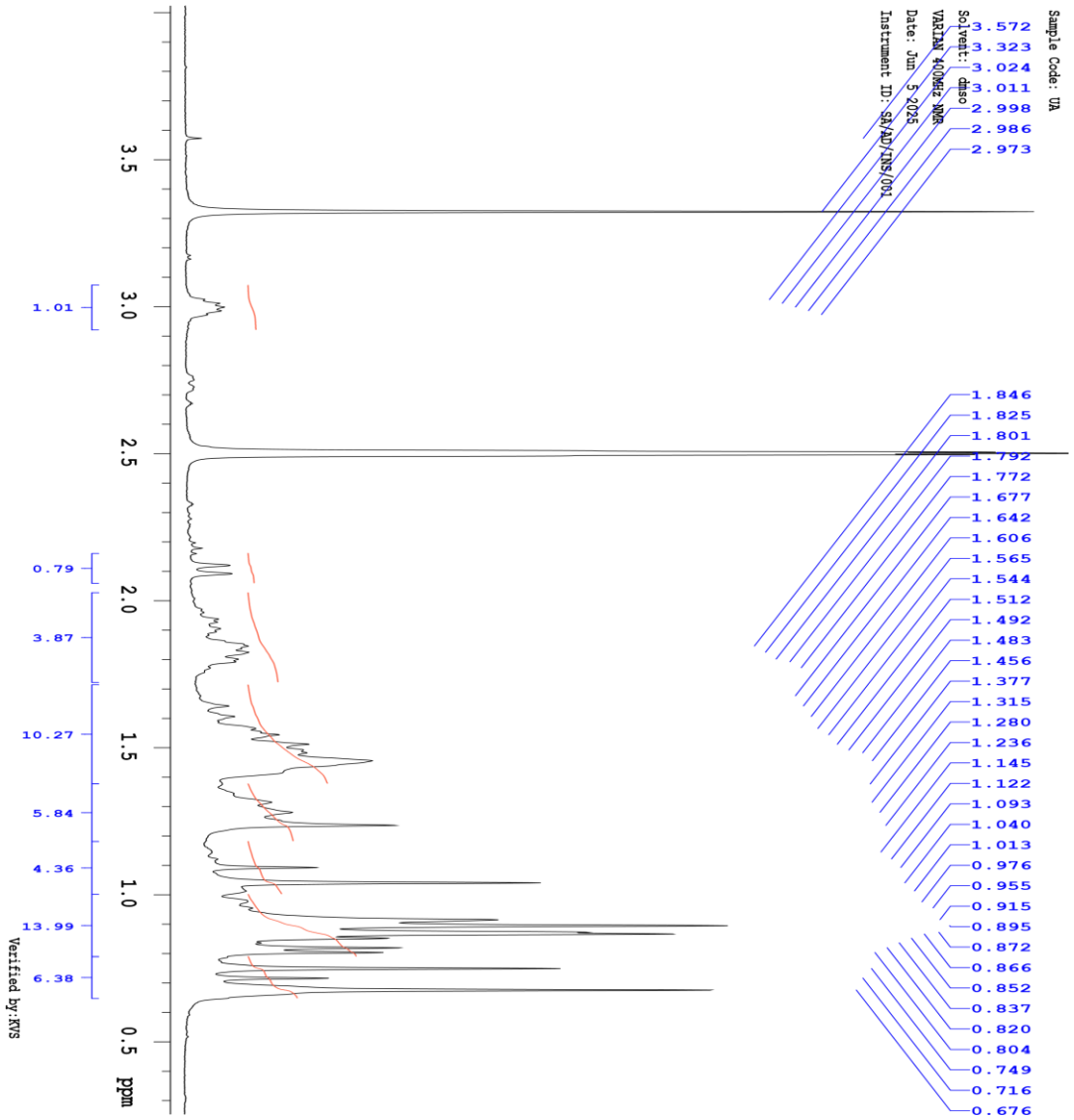

exp1 PROTON

SAMPLE PRESATURATION date Jun 52025 satmode n solvent dmso wet n file /home/varian/~ SPECIAL data/2025/Jun/UA_2~ temp not used 0250605_01/UA_PROT~ gain 30 ON_20250605_01.fid spin 20 ACQUISITION hst 0.008 sw 8802.8 pw90 13.000 at 3.722

alfa 10.000 np 65536 FLAGS fb 4000 il n bs 2 in n d1 1.000 dp y nt 128 hsnnct 22 PROCESSING TRANSMITTER lb 0.50 tn H1 fn not used sfrq 399.692 DISPLAY tof 1598.7 sp -798.7 tpwr 59 wp 8802.5 pw 6.500 rfl 798.9 DECOUPLER rfp 0 dn C13 rp -140.1 dof 0 lp 0 dm nnn PLOT decwave W40_GATB-0~ wc 268 12 sc 0 dpwr 35 vs 1793 dmf 29412 th 3 ai cdcph

Plotname: UA_PROTON_20250605_01_plot04 INDEX

No.	Frequency	PPM	Height
1	4787.2	11.977	6.5
2	2062.1	5.159	3.9
3	2049.7	5.128	9.8
4	1716.1	4.294	14.6
5	1711.0	4.281	15.3
6	1427.8	3.572	2.8
7	1328.2	3.323	131.7
8	1208.6	3.024	3.3
9	1203.5	3.011	5.6
10	1198.4	2.998	6.4
11	1193.6	2.986	5.9
12	1188.2	2.973	3.8
13	1001.5	2.506	125.7
14	999.9	2.502	166.0
15	998.0	2.497	122.5
16	870.7	2.178	2.9
17	847.6	2.121	7.2
18	836.3	2.092	7.5
19	787.7	1.971	2.9
20	783.4	1.960	3.2
21	774.5	1.938	5.4
22	770.2	1.927	5.3
23	761.3	1.905	5.8
24	757.3	1.895	5.1
25	752.7	1.883	3.9
26	737.7	1.846	10.1
27	729.4	1.825	10.1
28	720.0	1.801	8.5
29	716.2	1.792	8.1
30	708.1	1.772	4.2

31	670.3	1.677	2.7
32	656.3	1.642	7.0
33	642.1	1.606	8.0
34	625.7	1.565	11.2
35	617.1	1.544	14.8
36	604.2	1.512	19.4
37	596.4	1.492	18.6
38	592.6	1.483	19.1
39	581.9	1.456	29.3
40	550.2	1.377	6.0
41	525.5	1.315	13.7
42	511.8	1.280	16.9
43	494.0	1.236	32.9
44	457.8	1.145	4.4
45	448.4	1.122	5.3
46	436.8	1.093	20.7
47	415.9	1.040	55.3
48	404.8	1.013	9.7
49	390.1	0.976	10.0
50	381.7	0.955	10.7
51	365.9	0.915	48.7
52	357.8	0.895	84.3
53	348.7	0.872	62.6
54	346.3	0.866	75.8
55	340.6	0.852	31.7
56	334.5	0.837	12.0
57	327.7	0.820	33.6
58	321.3	0.804	31.0
59	299.5	0.749	58.4
60	286.4	0.716	22.4
61	270.3	0.676	81.7
62	0.0	0.000	73.0
63	-3.2	-0.008	3.3

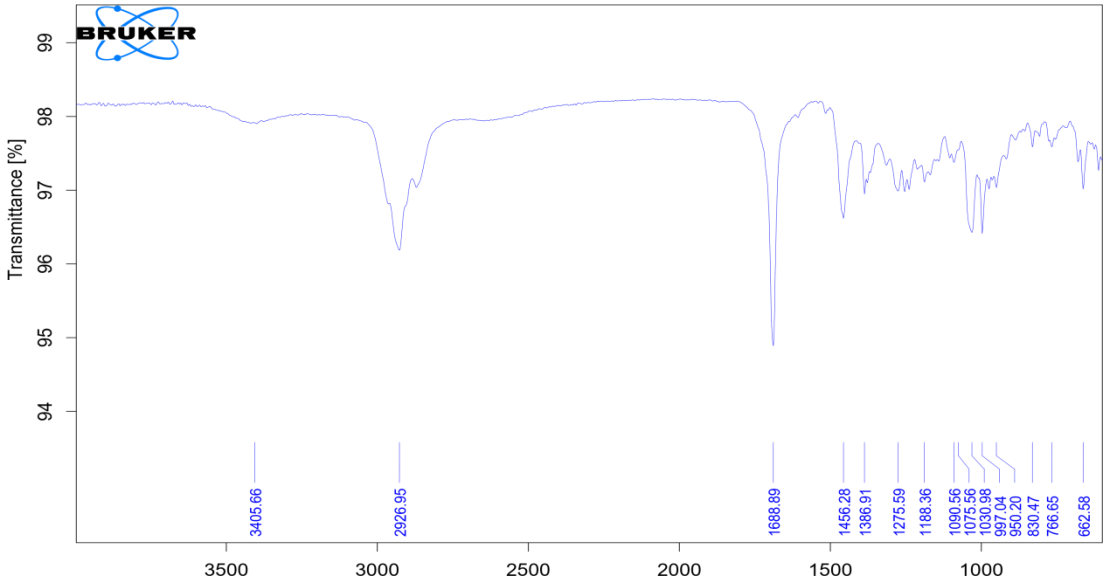

Wavwnumber cm-1

C:\Users\ADMIN\Documents\Bruker\OPUS_8.7.41\DATA\MEAS\UA.0	**UA**	**Powder**	**10-06-2025**

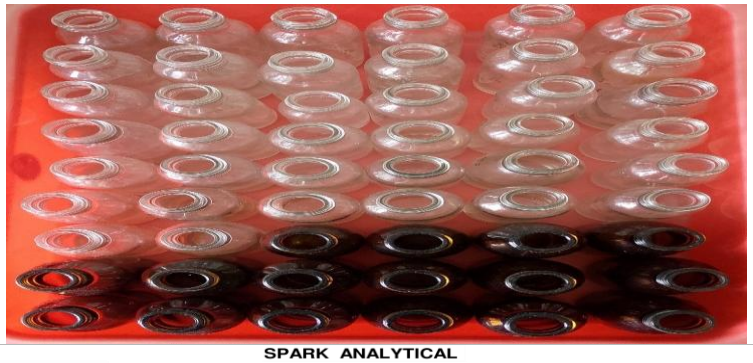

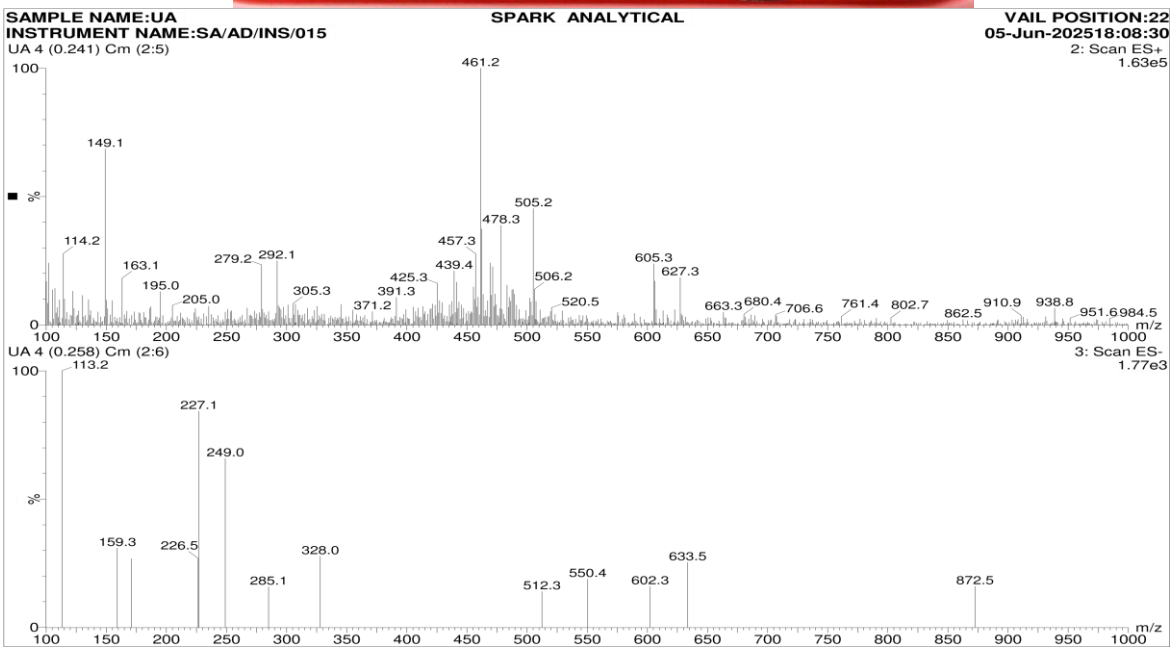

FIG:2-Fractions

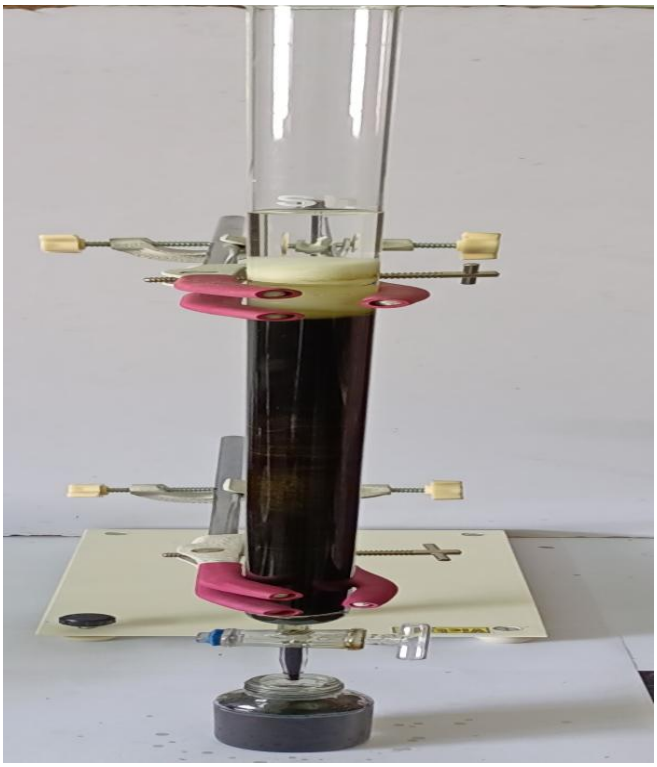

FIG:3-Column

4. MOLECULAR DOCKING:

Molecular docking as a key tool in structural molecular biology and computerassisted drug design. Ligand-protein docking aims to foretell the main mode(s) of ligandprotein interaction with proteins with known three-dimensional structures(35).

The molecular docking method can be used to mimic the atomic-level interaction between a small molecule and a protein, which enables us to define the behaviour of small molecules in the binding site of target proteins and to elucidate key biochemical processes(36). The docking procedure consists of two fundamental steps: the prediction of the ligand structure as well as its position and orientation within these sites (often known as pose) and the evaluation of the binding affinity(37).

The purpose of molecular docking is to anticipate the structure of the ligand-receptor complex using computational approaches(38). Docking can be accomplished in two

interdependent steps: first, by sampling conformations of the ligand in the active site of the protein; and second, by ranking these conformations using a scoring function. In an ideal situation, sampling algorithms should be able to duplicate the experimental binding mode, and the scoring function should rank it highest among all generated conformations(39.40). The objective of the scoring function is to distinguish between proper and wrong poses or active and inactive chemicals in a fair amount of time. However, scoring functions can be classified as force-field-based, empirical, or knowledge-based(41).

In this study, we calculated the sum of the non-bonded (electrostatics and van der Waals) interactions to determine the binding energy using scoring functions based on the Classical force field(42).

Preparation of the Protein:

Glycogen Synthase Kinase-3 (GSK-3), Angiotensin-Converting Enzyme (ACE), and Tumor Necrosis Factor-α Converting Enzyme (TACE) are critical targets involved in the regulation of inflammation, cardiovascular function, and immune responses(43). GSK-3 plays a pivotal role in inflammatory signaling and is associated with autoimmune conditions such as rheumatoid arthritis. ACE is well known for its role in hypertension but also contributes to vascular inflammation, while TACE regulates the release of pro-inflammatory cytokines such as TNF-α, making it a therapeutic target in chronic inflammatory diseases(44). The crystal structures of GSK-3 (PDB ID: IH8F), ACE (PDB ID: 1086), and TACE (PDB ID: 3LOT) were retrieved from the Protein Data Bank (https://www.rcsb.org/). All heteroatoms were removed, and polar hydrogen atoms were added to each protein to prepare them for molecular docking. These proteins were chosen for their relevance in inflammation-mediated diseases and their potential for therapeutic targeting through small molecule inhibitors(45).

Preparation of the Ligand – URSOLIC ACID

The structures of the synthesized compounds were drawn using ChemSketch software where the output is saved as .mol2 files. Then these compounds were saved in 3D form using UCSF chimera AutoDocksoftware(46). The ligand molecules were processed by the removal of water molecules and the addition of hydrogen bonds and charges. The charges were included as Amber ff14SB standard residues and in Gastregier form in non-standard residues(47).

Docking Using AutoDock Vina

The docking study was performed on a crystal structure of (IH8F(GSK3),1086(ACE),3LOT(TACE) using AutoDock Vina in UCSF chimera software, in which there is an online version of AutoDock provided by opal web service(48). This method of docking allows only a single compound to be docked at a time. The pre-optimized compounds were open and pre-processed similarly and converted to PDBQT format. All the torsion angles in the small molecules were set free so as to perform flexible docking(49). Grid box of size 75x 75x75 with a centre spacing of zero was defined along the x, y and z-axis. The grid box was adjusted to cover the active site of the protein. The analysis of binding and interaction of ligands with residues on active site was carried out by using Discovery studio 4.1(50).

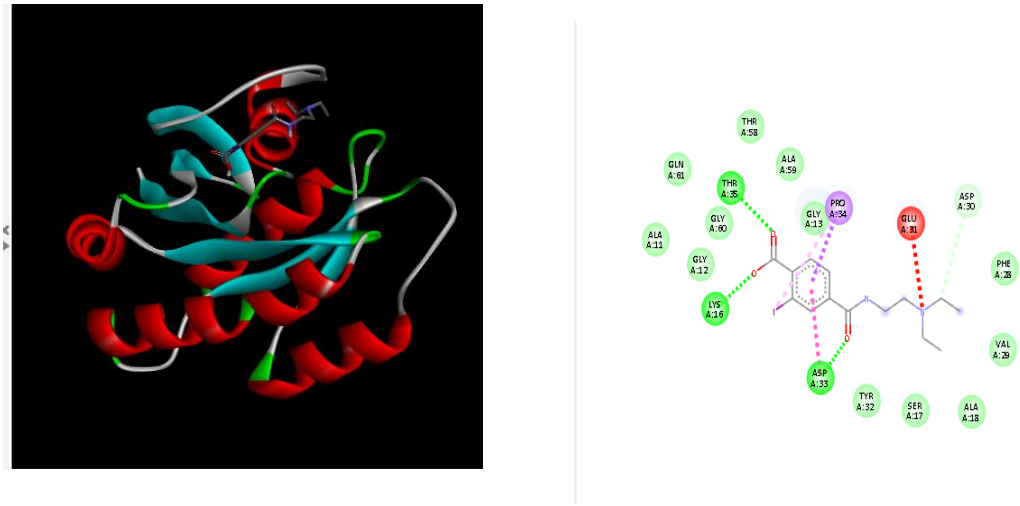

FIG:4-Docking image of ursolic acid with IH8F(GSK3)

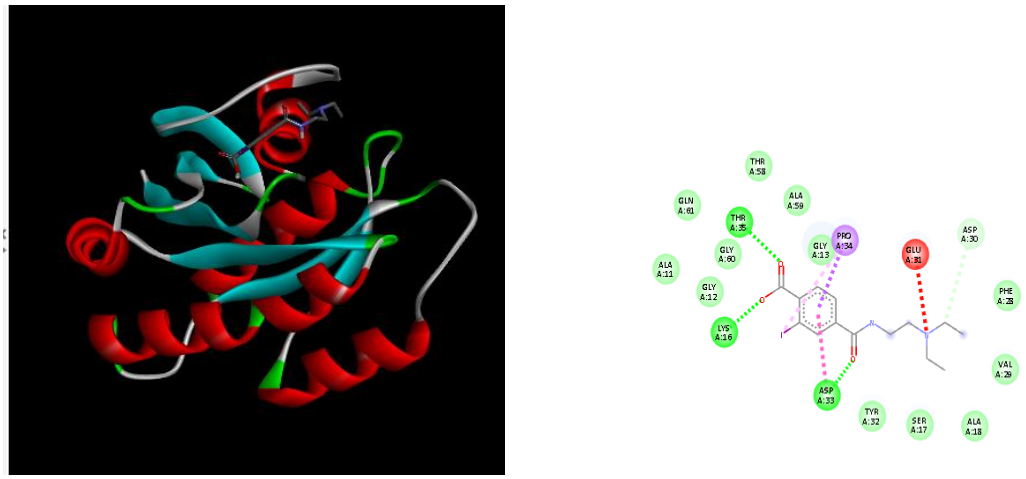

FIG:5- Docking image of ursolic acid with 1086(ACE)

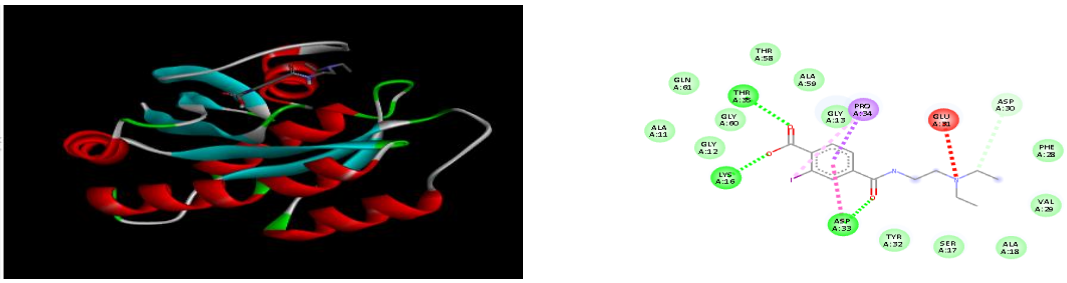

FIG:6-Docking image of ursolic acid with 3LOT(TACE)

5. RESULT AND DISCUSSION :

Column chromatography of the methanolic plant extract yielded multiple fractions. Among these, fractions 16–21 exhibited a single spot on TLC with consistent Rf values (0.58), indicating a chemically pure compound. These fractions were pooled, crystallized, and subjected to detailed spectral analysis. The isolated compound was a colorless solid with a melting point of 284–287°C, suggesting high purity.

FTIR analysis revealed strong absorption bands at 3405 cm^{-1} (–OH), 2926 cm^{-1} (–CH), 1688 cm^{-1} (C=O), and 1030 cm^{-1} (C–O), confirming the presence of hydroxyl and carboxylic acid functional groups. ^{1}H-NMR spectroscopy showed characteristic signals including δ 11.97 ppm (carboxylic proton), δ 5.12–5.15 ppm (vinyl proton), and δ 0.67–1.84 ppm (methyl and methylene groups), indicating a triterpenoid skeleton. ^{13}C-NMR displayed 30 distinct carbon resonances, including δ 178.56 (carboxylic carbon), δ 138.17 and 124.56 (olefinic carbons), and δ 76.80 (hydroxylated carbon), consistent with the structure of ursolic acid. Mass spectrometry confirmed the molecular ion peak at m/z 457.3 [M+1], supporting the molecular formula $C_{30}H_{48}O_3$.

Molecular Docking Studies:

The isolated ursolic acid was subjected to molecular docking against three critical targets implicated in neuroinflammation and Alzheimer's disease progression:

Glycogen Synthase Kinase-3 (GSK3; PDB ID: 1H8F)

Angiotensin-Converting Enzyme (ACE; PDB ID: 1O86)

Tumor Necrosis Factor-α Converting Enzyme (TACE; PDB ID: 3LOT)

GSK3, especially its β-isoform (GSK3β), plays a crucial role in Alzheimer's pathology by contributing to tau hyperphosphorylation, a hallmark of neurofibrillary tangles. ACE is involved not only in blood pressure regulation but also in the degradation of amyloid-beta (Aβ), the accumulation of which is central to Alzheimer's. TACE, also known as ADAM17, facilitates the release of pro-inflammatory cytokines like TNF-α, which exacerbate neuronal damage in Alzheimer's via microglial activation.

Using AutoDock Vina integrated in UCSF Chimera, docking studies showed that ursolic acid exhibits significant binding affinity toward all three targets. It forms stable hydrogen bonds and hydrophobic interactions within the active sites of GSK3, ACE, and TACE, with optimal orientation due to full torsional flexibility during docking.

Strongest interaction was observed with TACE, suggesting that ursolic acid could suppress TNF-α activation and thereby reduce neuroinflammation.

Binding with GSK3 indicates potential inhibition of tau hyperphosphorylation, a pivotal process in Alzheimer's neurodegeneration.

ACE interaction supports a possible role in modulating amyloid-beta levels and cerebral blood flow, both key components in Alzheimer's pathology.

The docking data suggest that ursolic acid may serve as a multi-target neuroprotective agent capable of modulating interconnected pathways in Alzheimer's disease, including tau pathology (via GSK3), neuroinflammation (via TACE), and amyloid metabolism (via ACE). Its ability to engage with all three targets highlights its potential utility as a natural scaffold for developing Alzheimer's therapeutics.

6. CONCLUSION:

In this study, **ursolic acid**, a pentacyclic triterpenoid compound, was successfully isolated from a medicinal plant extract and structurally characterized using advanced analytical techniques including **FTIR, ^{1}H-NMR, ^{13}C-NMR, and mass spectrometry**. The spectral data confirmed the presence of characteristic functional groups and structural features consistent with ursolic acid, validating the reliability of the extraction and purification process.

To evaluate its therapeutic relevance to **Alzheimer's disease**, ursolic acid was further assessed through **molecular docking studies** against three inflammation- and neurodegeneration-related targets:

Glycogen Synthase Kinase-3 (GSK3, PDB ID: 1H8F) – involved in tau hyperphosphorylation,

Angiotensin-Converting Enzyme (ACE, PDB ID: 1O86) – linked to amyloid-beta degradation and cerebrovascular dysfunction,

Tumor Necrosis Factor-α Converting Enzyme (TACE, PDB ID: 3LOT) – responsible for TNF-α release and neuroinflammation.

The docking results revealed **high binding affinity** of ursolic acid to all three protein targets. These interactions suggest that ursolic acid may modulate **key pathological mechanisms in Alzheimer's disease**, including **tau aggregation, neuroinflammatory signaling, and amyloid-beta metabolism**.

Overall, the study demonstrates that **ursolic acid exhibits multi-target potential** and could serve as a promising **lead compound for neuroprotective drug development**. The integration of natural compound isolation with **in silico docking analysis** offers a valuable strategy for identifying candidates targeting **complex diseases like Alzheimer's**, where multi-pathway modulation is essential. Further **in vivo and clinical studies** are warranted to explore and validate the neurotherapeutic efficacy of ursolic acid

REFERENCES

[1] Kofi Annan, Nora Jackson, Rita A. Dickson, George H. Sam" Gustav Komlaga, Acaricidal effect of an isolate from Hoslundiaoppositavahl against Amblyomma variegatum (Acari: Ixodidae), Pharmacognosy Research 2011,3, 185.

[2] Liu J. Pharmacology of oleanolic acid and ursolic acid. J Ethnopharmacol. 1995;49(2):57-68.

[3] Ikeda Y, Murakami A, Ohigashi H. Ursolic acid: an anti- and pro-inflammatory triterpenoid. Mol Nutr Food Res. 2008;52(1):26-42.

[4] Ríos JL, Francini F. Inflammatory properties of triterpenoids. Phytother Res. 2005;19(9):703-12.

[5] Shanmugam MK, Dai X, Kumar AP, Tan BK, Sethi G, Bishayee A. Ursolic acid in cancer prevention and treatment: molecular targets, pharmacokinetics and clinical studies. BiochemPharmacol. 2013;85(11):1579-87.

[6] Sampath C, Rashid MR, Sang S, Ahmedna M. Bioactive phytochemicals in anti-inflammatory herbs. Food Funct. 2018;9(11):5431-63.

[7] Satyanarayana T, Manohar RD. Ursolic acid–a versatile pentacyclic triterpenoid: pharmacological and analytical aspects. J Pharm Sci Res. 2015;7(8):248-54.

[8] Rakesh K, Anil M, Megha G. Role of GSK-3 in inflammation and its inhibitors as future therapeutic targets. Inflamm Res. 2020;69(3):203-16.

[9] Bernstein KE, Khan Z, Ghosh S, et al. ACE and ACE2: their role in inflammation and fibrosis. Curr Opin Nephrol Hypertens. 2018;27(3):203-10.

[10] Garton KJ, Gough PJ, Blobel CP, et al. Tumor necrosis factor-alpha converting enzyme (TACE/ADAM17) in inflammation and cell signaling. J Biol Chem. 2001;276(43):40241-7.

[11] Morris GM, Huey R, Lindstrom W, et al. AutoDock4 and AutoDockTools4: automated docking with selective receptor flexibility. J Comput Chem. 2009;30(16):2785-91.

[12] Trott O, Olson AJ. AutoDock Vina: improving the speed and accuracy of docking with a new scoring function. J Comput Chem. 2010;31(2):455-61.

[13] Meng XY, Zhang HX, Mezei M, Cui M. Molecular docking: a powerful approach for structure-based drug discovery. Curr Comput Aided Drug Des. 2011;7(2):146-57.

[14] Pettersen EF, Goddard TD, Huang CC, et al. UCSF Chimera–a visualization system for exploratory research and analysis. J Comput Chem. 2004;25(13):1605-12.

[15] Biovia DS. Discovery Studio Modeling Environment, Release 4.1. San Diego: Dassault Systèmes; 2015.

[16] Jones G, Willett P, Glen RC. Molecular recognition of receptor sites using a genetic algorithm with a description of desolvation. J Mol Biol. 1995;245(1):43-53.

[17] Ekins S, Mestres J, Testa B. In silico pharmacology for drug discovery: methods for virtual ligand screening and profiling. Br J Pharmacol. 2007;152(1):9-20.

[18] Berman HM, Westbrook J, Feng Z, et al. The Protein Data Bank. Nucleic Acids Res. 2000;28(1):235-42.

[19] Tautenhahn R, Cho K, Uritboonthai W, Zhu ZJ, Patti GJ, Siuzdak G. An accelerated workflow for untargeted metabolomics using spectral processing and statistical analysis. Anal Chem. 2012;84(11):5071-9.

[20] Kumar S, Pandey AK. Chemistry and biological activities of flavonoids: an overview. ScientificWorldJournal. 2013;2013:162750.

[21] Silva T, Oliveira C, Borges F. Cinnamic acid derivatives as promising anti-inflammatory agents. Curr Med Chem. 2012;19(25):4638-50.

[22] Hu Y, Sun H, Xu F, et al. Ursolic acid derivatives for the treatment of inflammation and cancer: a patent review. Expert Opin Ther Pat. 2020;30(6):423-41.

[23] Yen GC, Duh PD, Tsai HL. Antioxidant and pro-oxidant properties of ascorbic acid and gallic acid. Food Chem. 2002;79(3):307-13.

[24] Panda SK, Swain KC. Phytochemical screening and GC-MS analysis of leaf extract of Ocimum sanctum L. Int J Curr Microbiol Appl Sci. 2011;5(1):1-8.

[25] Trivedi R, Tiwari RK, Parouha YK. Synthesis and characterization of ursolic acid and its derivatives. Indian J Chem B. 2013;52:1324-8.

[26] Yang M, Cheng X, Chen J, et al. Ursolic acid attenuates LPS-induced acute lung injury in mice. Inflamm Res. 2013;62(3):217-26.

[27] Iwata K, Matsuo K, Iida M, et al. Ursolic acid exerts anti-inflammatory effects on skin cells via the MAPK and NF-κB pathways. J Dermatol Sci. 2011;62(3):204-12.

[28] He W, Li Y, Guan H, Xiong Y, Lu Y. Therapeutic potential of ursolic acid against inflammation and cancer. Cancer Lett. 2019;460:1-12.

[29] Singh GB, Singh S. Anti-inflammatory and antimicrobial activities of triterpenoids from Eucalyptus globulus. Fitoterapia. 2005;76(4):329-32.

[30] Bharathi E, Radhika B. Isolation and structural elucidation of ursolic acid from Ocimum sanctum leaves. Int J Pharm Sci Res. 2013;4(7):2586-9.

[31] Zhang Y, Liu Y, Wang T, et al. Ursolic acid inhibits breast cancer progression through repressing cancer stemness via IL-6/STAT3 pathway. Oncotarget. 2017;8(38):70722-33.

[32] Wang X, Li F, Yang X, et al. Anti-inflammatory effects of ursolic acid: a review. Chin J Nat Med. 2020;18(11):803-20.

[33] Yang Y, Liu M, Wu H, et al. Pharmacokinetics and tissue distribution of ursolic acid in rats. J Ethnopharmacol. 2013;146(3):841-6.

[34] Moghadasian MH. Clinical pharmacology of plant sterols. Cardiovasc Ther. 2009;27(2):117-25.

[35] Xu H, Wang Y, Liu C, et al. Ursolic acid modulates NF-κBsignaling in inflammation: a review of preclinical evidence. Front Pharmacol. 2021;12:719693.

[36] Wang C, Wu S, Tu Y, et al. Anti-inflammatory triterpenoids from Rosmarinus officinalis. J Agric Food Chem. 2014;62(19):4517-25.

[37] Fan S, Zhang C, Luo T, et al. Anti-inflammatory effects of ursolic acid via suppression of NF-κB and MAPK pathways in LPS-stimulated RAW 264.7 macrophages. Int Immunopharmacol. 2019;67:223-31.

[38] Rashmi R, Satish V. FTIR and NMR characterization of phytocompounds from medicinal plants. J Pharm Sci Res. 2018;10(4):798-802.

[39] Zhou W, Hu J, Yu L, et al. Targeting GSK3β for treating inflammatory diseases. Front Pharmacol. 2021;12:755034.

[40] Mahato SB, Kundu AP. 13C NMR spectra of pentacyclic triterpenoids – a compilation. Phytochemistry. 1994;37(6):1517-75.

[41] Saini N, Singh D, Sandhu D. FTIR and NMR studies of anti-inflammatory compounds. Int J Pharm Sci Rev Res. 2015;30(2):56-61.

[42] Ghosh R, Chakraborty R, Raychaudhuri U, et al. Role of phytochemicals in cancer chemoprevention. J Food Sci Technol. 2011;48(5):495-505.

[43] Patil S, Patil V, Kadam V. Molecular docking: a review. World J Pharm Res. 2015;4(7):1481-96.

[44] Zhou L, He H, Liu J, et al. Anti-inflammatory and anti-apoptotic effects of ursolic acid on LPS-induced acute kidney injury. Int Immunopharmacol. 2020;89:107040.

[45] Nagao T, Okabe H, Arai I, et al. Search for naturally occurring substances to prevent cancer–anti-tumor promoting activity of triterpenoids. Cancer Lett. 1989;48(2):179-85.

[46] Xu W, Chen X, Shen Y. Anti-inflammatory activity of natural pentacyclic triterpenes. Chin J Nat Med. 2015;13(1):25-35.

[47] Prabhakar PK, Doble M. A target based therapeutic approach towards diabetes mellitus using medicinal plants. Curr Diabetes Rev. 2008;4(4):291-308.

[48] Kim SH, Lee SE, Oh H, et al. Anti-inflammatory and antinociceptive effects of ursolic acid isolated from Corni fructus. Arch Pharm Res. 2011;34(12):2033-41.

[49] Zhao J, Liu J, Cheng H, et al. Ursolic acid exerts neuroprotective effects via Nrf2 signaling. Front Pharmacol. 2020;11:558034.

[50] Aguilar JL, Rojas P, Marcelo A, et al. Anti-inflammatory activity of herbal extracts in macrophages. J Ethnopharmacol. 2002;81(2):271-6.

[51] Lam PY, Jadhav PK. Bioactive natural products as leads in drug discovery. J Med Chem. 2014;57(19):7873-95